

# Tunable Bands in 1D Fractional Quantum Media

Brenden R. Guyette<sup>1,2</sup>, Joshua M. Lewis<sup>1,2</sup>, and Lincoln D. Carr<sup>1,2,3</sup>

<sup>1</sup>*Quantum Engineering Program,*

*Colorado School of Mines, Golden, CO 80401, U.S.A.*

<sup>2</sup>*Department of Physics, Colorado School of Mines,  
Golden, CO 80401, U.S.A.*

<sup>3</sup>*Department of Applied Mathematics and Statistics,  
Colorado School of Mines, Golden, CO 80401, U.S.A.*

(Dated: November 25, 2025)

Fractional calculus [1, 2] has become an essential framework in geophysics [3], optics [4, 5], and biological systems [6, 7] to capture long-range correlations and anomalous transport. In this article, we extend the success of fractional calculus in physical models to explore a particle in a periodic potential, where the Schrödinger equation is extended to its fractional form [1, 2]. This framework enables us to study how the Lévy index  $q$  governs the formation and inversion of energy bands, offering a pathway to engineer new physical behaviors and device functionalities by tuning  $q$  in periodic quantum systems. We solve the fractional Schrödinger equation (FSE) for periodic rectangular potentials of varying height  $V_0$ , barrier thickness  $L$ , and well width  $W$  using an imaginary-time evolution algorithm [8], and supplement the discrete energy dispersion through Gaussian process regression [9]. This analysis reveals a qualitative shift in the system's band structure at  $q = 2$ , separating into distinct regimes of dispersion that define behavior for  $q > 2$  and  $q < 2$ . For  $q > 2$ , the energy bands undergo an inverting transformation as symmetric minima emerge within the first Brillouin zone and shift from  $k = 0$  toward  $k = \pm\pi/a$  with increasing  $q$ . These degenerate minima define a Bloch-momentum qubit, suggesting an analog to valley degrees of freedom used in valleytronics [10]. The response of the ground band to inversion scales with fractional order as  $V_0^{-0.28 \pm 0.05} L^{-0.34 \pm 0.08} W^{-0.49 \pm 0.06}$ , indicating a tunable sensitivity to potential geometry. In contrast, for  $q < 2$ , the effective mass near  $k = 0$  decreases exponentially with  $q$ , with the rate set jointly by  $V_0$ ,  $L$ , and  $W$ . As  $q \rightarrow 1$ , this dependence becomes dominated by the fractional order itself, yielding a universal effective mass of  $0.15 \pm 0.01$  with less than 0.06 variance across all tested potentials. These results demonstrate that the Lévy index serves as a tunable degree of freedom in quantum periodic systems, capable of driving band inversion, modulating the band gap, and reshaping carrier dynamics through effective-mass control.

## I. INTRODUCTION

Fractional calculus generalizes differentiation and integration to noninteger orders  $q$  [1, 2], providing a natural framework for modeling nonlocality and memory effects. Unlike classical differential operators that act locally and assume smooth, short-ranged dynamics, fractional derivatives encode power-law correlations and long-range interactions. As a result, they have become central in describing anomalous transport, scaling phenomena, and collective behavior in complex systems.

Fractional models have found broad application across the sciences. In geophysics, fractional diffusion equations describe subdiffusive transport in porous media, where heterogeneous microstructures induce spatial correlations and memory effects [3]. Optical systems employ the fractional Schrödinger equation to characterize light propagation in photonic lattices and waveguides that exhibit nonlocal or nonparaxial response [4, 5]. Biological transport processes, from intracellular motion to animal foraging, reveal Lévy-flight dynamics and heavy-tailed step-length distributions that reflect the same anomalous scaling [6, 7]. This article implements the physics of Lévy-driven anomalous diffusion in periodic one-dimensional quantum systems governed by the frac-

tional Schrödinger equation.

Quantum dynamics are inherently probabilistic, governed by wavefunctions that evolve through a superposition of possible particle paths. Traditionally, these paths correspond to Brownian motion with Gaussian-distributed step lengths [11–13]. However, in complex, disordered, or fractal media, transport often deviates from this Gaussian limit and follows Lévy statistics, where rare but large steps give rise to anomalous diffusion [1, 2, 14, 15].

To describe such anomalous quantum transport, the fractional Schrödinger equation (FSE) extends the classical framework by incorporating fractional derivatives derived from Lévy flight path integrals [1, 2]. This generalization introduces a fractional order  $q$  that defines the Lévy index of the system and the diffusive nature of its quantum states.

When a quantum particle experiences a periodic potential, its energy spectrum forms bands, with allowed energy states, or eigenstates, described by Bloch's theorem [16]. These bands follow a repeating periodic structure within the Brillouin zone in quasi-momentum. These bands repeat periodically within the Brillouin zone in quasi-momentum, or  $k$ -space. Altering a particle's diffusive nature modifies the allowed states, resulting in a

topological transition of the ground band. We examine this transition for its potential use in computation, where valleytronics exploits naturally occurring valleys in band structure as informational degrees of freedom [10], and in transport phenomena, where the effective mass governs carrier mobility [17].

Despite the growing use of fractional models across disciplines, their role in shaping quantum band structure within periodic systems remains largely unexplored. In this article, we numerically investigate how the fractional order  $q$  shapes the band structure of a one-dimensional periodic array of rectangular wells. Two distinct regimes emerge: for  $q < 2$ , the lowest-energy state exhibits an exponential reduction in effective mass, while for  $q > 2$ , the ground band undergoes inversion with degenerate minima forming a Bloch-momentum qubit. These findings reveal that fractional order is a physical degree of freedom that can be engineered to tune band inversion and effective mass within periodic quantum systems.

## II. FRACTIONAL SCHRÖDINGER EQUATION AND SIMULATION METHOD

The time-dependent FSE in one dimension is expressed as

$$i\hbar \frac{\partial \psi(x, t)}{\partial t} = -\frac{\hbar^2}{2m} \left( C_q \frac{\partial^q \psi(x, t)}{\partial x^q} \right) + V(x)\psi(x, t),$$

where  $\psi(x, t)$  is the wavefunction,  $V(x)$  is the potential energy, and  $C_q$  is a scaling coefficient with units  $\text{m}^{q-2}$  to maintain dimensional consistency with the standard kinetic term. The fractional derivative,  $\partial^q \psi / \partial x^q \equiv \partial^q \psi$  obeys

$$\mathcal{F}\{\partial^q \psi\}(x) = -|k|^q \tilde{\psi}(k)$$

for  $q > 0$ , where  $\tilde{\psi}$  is the Fourier transform of  $\psi$  [18]. In the limit  $q \rightarrow 2$ , this operator reduces to the standard Laplacian, and Equation (II) recovers the conventional time-dependent Schrödinger equation.

Assuming a stationary-state solution of the form  $\psi(x, t) = \phi(x)e^{-iEt/\hbar}$ , the time-dependent FSE reduces to its time-independent form,

$$E\phi(x) = -\frac{\hbar^2}{2m} \left( C_q \frac{\partial^q}{\partial x^q} \right) \phi + V(x)\phi.$$

which defines the energy eigenstates  $\phi(x)$  and corresponding eigenvalues  $E$ .

We consider a one-dimensional system subject to a spatially periodic rectangular potential  $V(x) = V(x+a)$  with period  $a = L+W$ , consisting of alternating wells of width  $W$  and barriers of width  $L$ . This configuration provides a minimal framework to investigate how the fractional order  $q$  modifies the electronic band structure.

Because the potential is periodic, Bloch's theorem applies [19], and the fractional derivative preserves this periodicity. Consequently, the eigenfunctions of the Hamiltonian can be written as

$$\psi_k(x) = e^{ikx} u_k(x), \quad u_k(x+a) = u_k(x),$$

where  $k$  is the Bloch wavevector and  $u_k(x)$  is periodic with the same period as the potential.

The fractional Schrödinger equation is solved numerically using an imaginary-time evolution scheme implemented via the Fourier split-step method [8]. Symmetry-based filtering, employing both parity and translational invariance, is incorporated to improve the precision and efficiency of the fractional Laplacian evaluation. For consistency with established models, we evaluate the case  $q = 2$ , corresponding to the standard Schrödinger equation. In this limit, the computed band structure reproduces the known results for periodic rectangular wells with an eigenstate energy convergence of magnitude  $10^{-15}$ .

From the computed energy dispersion  $E(k)$ , the curvature of the band determines the particle's effective mass, defined as

$$\frac{1}{m^*} = \left. \frac{d^2 E(k)}{dk^2} \right|_{k=k_0},$$

where  $k_0$  denotes the point of expansion in reciprocal space. The second derivative is evaluated numerically using a central finite-difference method applied to the discrete energy spectrum [17].

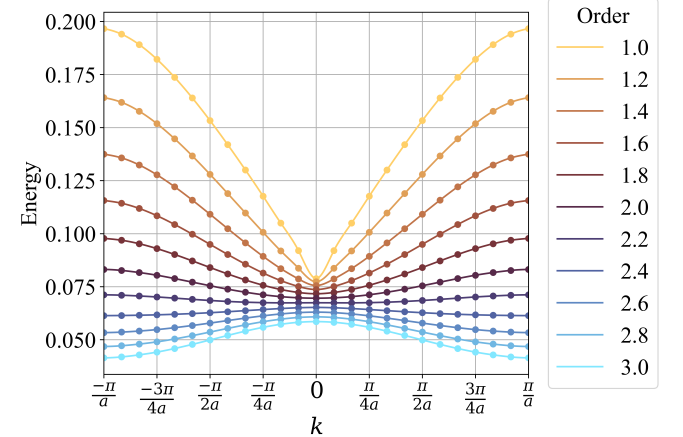


FIG. 1. Ground-band evolution within the first Brillouin zone as the fractional order  $q$  varies from 1.0 to 3.0. For  $q < 2$ , the band sharpens around  $k = 0$ , corresponding to a lower effective mass of the ground state. For  $q > 2$ , the band undergoes inversion: new minima emerge symmetrically about  $k = 0$  and migrate toward the zone edge, merging at  $k = \pi/a$  as inversion completes.

Figure 1 plots the ground band transformation within the first Brillouin zone as  $q$  varies from 1.0 to 3.0. This

ground-band transformation is present in many potentials, where the variance in  $W$ ,  $L$ , and  $V_0$  separately affect the transformation. Varying the fractional order  $q$ , within the range  $1 < q < 3$ , manifests two distinct regions of energy band transformation separated by  $q = 2$ . For  $q < 2$ , the curvature of the ground band near  $k=0$  increases, indicating a reduction in the effective mass. In contrast, for  $q > 2$ , the band inverts:  $k = 0$  becomes a local maximum, and the minima shift to symmetric points  $\pm k_{\min}$ , where  $E(k_{\min}) = \min(E(k))$  within the first Brillouin zone. As  $q$  continues to increase, they move continuously toward the zone boundary, reaching  $k_{\min} = \pi/a$  when the inversion is complete. Further increasing  $q$  steepens the band, with the energy at  $k = 0$  increasing.

### III. BEHAVIOR FOR $q > 2$

Beyond the classical limit of  $q = 2$ , the fractional order induces a topological transformation of the ground band, converting the central curvature into a local maximum and generating symmetric minima that define a new quantum degree of freedom. This inversion breaks the system's  $\mathbb{Z}_2$  symmetry [20], giving rise to a pair of degenerate states at opposite quasi-momenta that can serve as a Bloch-momentum qubit [21]. The qubit exists in re-

ciprocal space, with logical states distinguished by the sign of  $k$ . To explore how this qubit may be controlled, we draw an analogy to valleytronics [10], where information is encoded in  $k$ -space valleys whose separation and energy can be tuned by material parameters.

Band inversion is geometry dependent, with the potential parameters  $V_0$ ,  $L$ , and  $W$  setting the scale for its onset and completion. Increasing any of these parameters shifts the quasi momentum separation of the emergent minima to larger values for a fixed  $q > 2$ , indicating that the valley spacing of the Bloch-momentum qubit can be tuned by the potential geometry. Consequently, the fractional order at which the ground band completes inversion depends on these parameters. Figure 2 illustrates this dependence by comparing two ground-band transformations, one for a reference potential and another with  $V_0$  doubled.

Figure 3 shows the variation of local minima as the barrier width  $L$  varies. To approximate a continuous  $k$ -space without increasing computational cost, we employed Gaussian process regression (GPR) [9] to interpolate the discrete energy states, effectively reproducing the ground band of a system with many more wells. For the present case, the  $k$ -space sampling was increased by a factor of twelve (301 points instead of 25), enabling accurate identification of the minima within the ground band. We then fit the positions of these minima to a power law to estimate  $q$  when  $k_{\min} = \pm\pi/a$ .

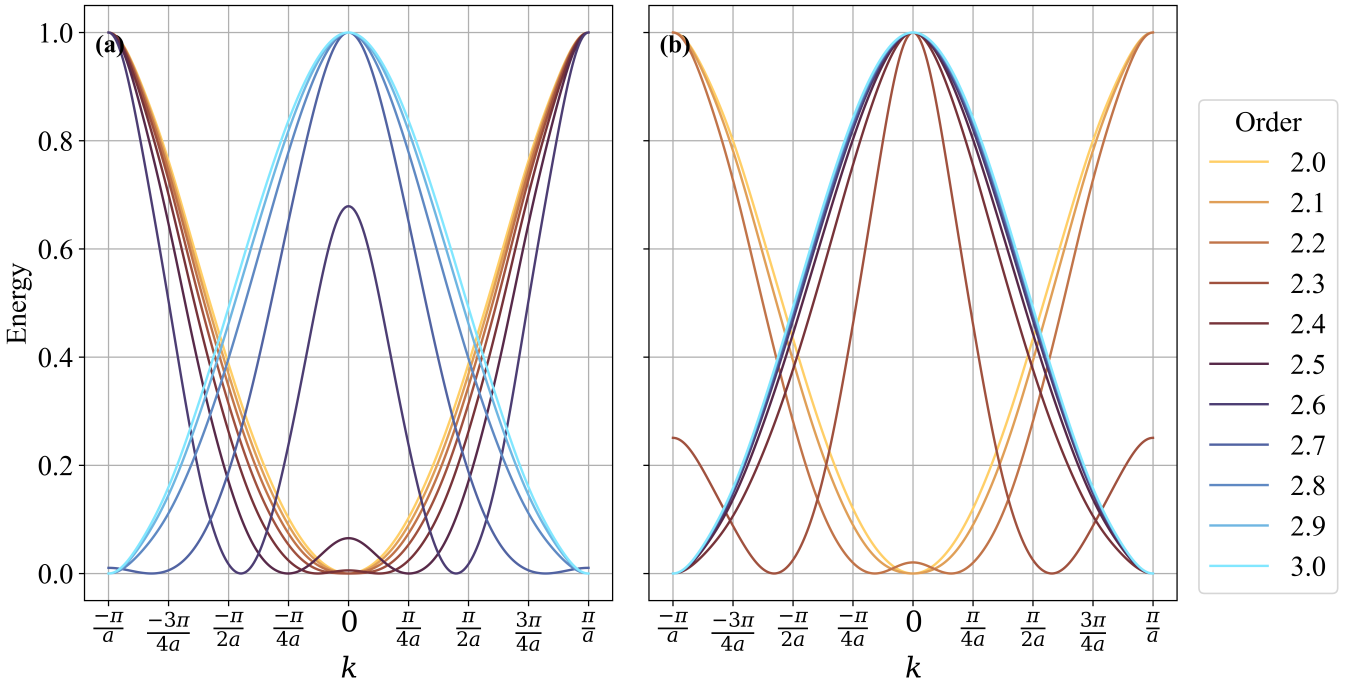


FIG. 2: Ground band tuning from fractional order 2.0 to 3.0. Two different cases are shown: (a) reference potential and (b) increased well height. Amplifying  $V_0$  increases the ground band's sensitivity to inversion monotonically across fractional orders. (a) Referential case, the ground band finishes inversion between orders 2.8 and 2.9. (b) Increased potential height ( $V_0$ ), the ground band finishes inversion around order 2.3.

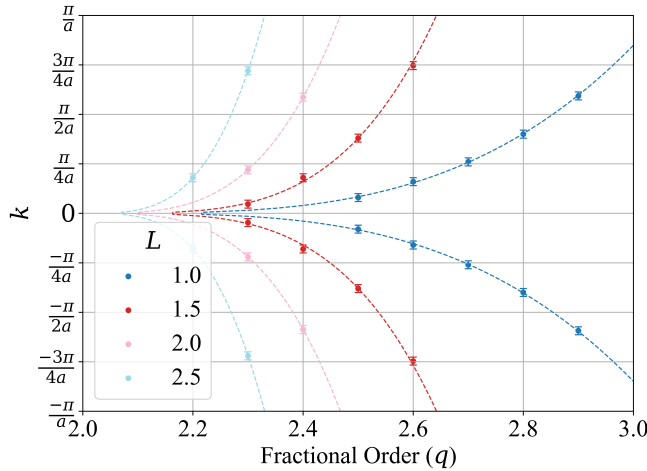
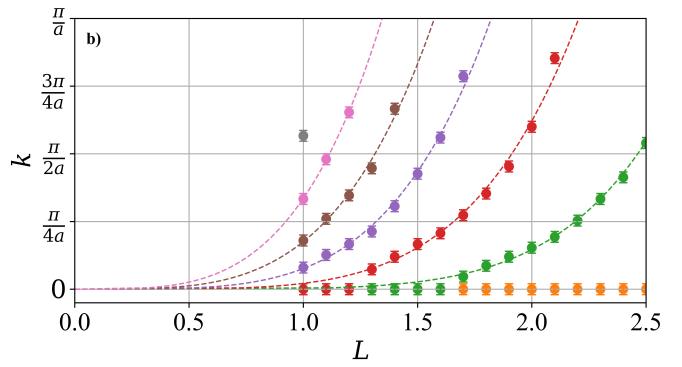
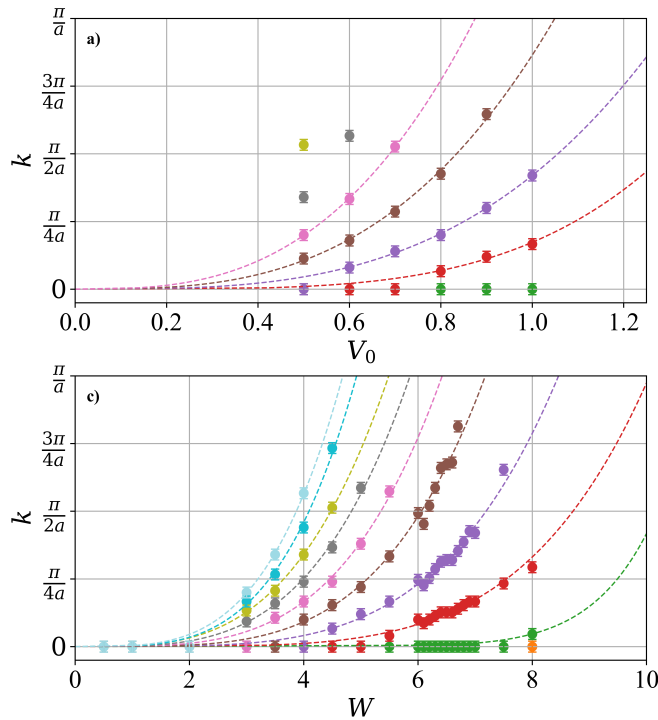


FIG. 3. Gaussian process regression (GPR) interpolation of the ground band to approximate a continuous  $k$ -space and capture the shifting of band minima. Points denote the positions of the ground band minima obtained from the GPR, and dashed curves are power-law fits showing how the minima shift with fractional order  $q$  for different potential parameters ( $V_0, L, W$ ). The intersection of each fit with  $k = \pm\pi/a$  marks the fractional order at which the ground band of a particle in a periodic rectangular potential completes its inversion scales as  $q \propto V_0^{-0.28 \pm 0.05} L^{-0.35 \pm 0.08} W^{-0.49 \pm 0.06}$  for  $q > 2$ .

From the collection of fractional orders  $q$  marking

the completion of band inversion for each set of potential parameters, we determined the proportionality governing inversion sensitivity by fitting a power law to the variation of  $q$  with  $V_0$ ,  $L$ , and  $W$ . Fits were retained only when the coefficient of determination satisfied  $0.9 < R^2 < 1.0$ , and any data points with a z-score greater than 3 were excluded as outliers. The mean exponents and their standard deviations were then computed from the accepted fits. The fractional order at which the ground band of a particle in a periodic rectangular potential completes its inversion scales as  $q \propto V_0^{-0.28 \pm 0.05} L^{-0.35 \pm 0.08} W^{-0.49 \pm 0.06}$  for  $q > 2$ .

This scaling relationship shows that the position of the energy band minima in  $k$ -space for  $q > 2$  can be tuned without altering the system periodicity. Adjusting the potential height  $V_0$  modifies the quasi-momentum spacing between extrema, enabling control of the valley separation at a fixed lattice period. Because band inversion depends on both  $q$  and the potential geometry, it can also be driven by varying  $L$ , or  $W$  while holding  $q$  constant above 2. Figure 4 demonstrates this tunability, showing that inversion can be induced or enhanced at a constant fractional order by adjusting individual potential parameters.



Fractional Order ( $q$ )											
●	2.0	●	2.6	●	2.1	●	2.7	●	2.2	●	2.8
●	2.3	●	2.8	●	2.4	●	2.9	●	2.5	●	3.0

FIG. 4: Tuning of the ground band minima at fixed fractional order  $q > 2$ . Varying the potential parameters  $V_0$ ,  $L$ , and  $W$  shifts the location of the minima in  $k$ -space (only  $0 \leq k \leq \pi/a$  is shown). The fitted curves yield the scaling exponents that characterize inversion sensitivity, with the fractional order at which inversion completes scaling as  $q \propto V_0^{-0.28 \pm 0.05} L^{-0.35 \pm 0.08} W^{-0.49 \pm 0.06}$ .

This inversion leaves a measurable imprint on the interband structure. When the first excited band does not invert concurrently, the band gap  $\Delta(q)$  exhibits a qualitative change. Before inversion,  $\Delta(q)$  grows monotonically with  $q$ . After inversion completes, the  $q$ -sensitivity weakens, producing a kink at the inversion point. Representative  $\Delta(q)$  curves may be seen in Figure 5.

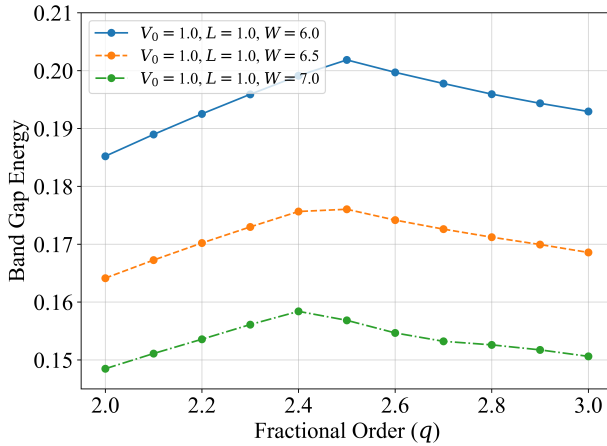


FIG. 5. Band gap  $\Delta(q)$  for three well widths  $W$ . A kink appears when only the ground band inverts, and its location shifts with  $W$ . Post-inversion,  $\Delta(q)$  shows reduced  $q$ -sensitivity.

Directness of the band gap is set by the  $k$ -alignment of the band-edge extrema. The gap is direct if the ground-band maximum and first-excited-band minimum occur at the same  $k$ , otherwise it is indirect. Direct gaps enable momentum-conserving optical transitions and strong radiative coupling, while indirect gaps require phonon assistance, suppressing emission and altering carrier relaxation pathways [22, 23]. Increasing  $q$  switches directness in some geometries, while others preserve it across  $q$ . The inversion of the first excited band follows a similar trend to that of the ground band; that is, taller potentials, thicker barriers, and more spaced wells promote inversion, but detailed proportionalities were not extracted.

Ground-band inversion for  $q > 2$  reorganizes the dispersion, results in a Bloch momentum qubit, and imprints a kink in  $\Delta(q)$  when only the ground band inverts. Geometry tunes the valley spacing at fixed  $q$  and shifts the inversion point, consistent with the observed  $V_0$ ,  $L$ ,  $W$  trends. These controls let  $q$  and geometry co-define qubit addressability and the directness of the gap, which set optical coupling and relaxation pathways [22, 23]. Together, they establish  $q$  as a practical axis of band-structure control for 1D devices.

#### IV. BEHAVIOR FOR $q < 2$

For  $q < 2$ , the dispersion hardens near  $k = 0$ : the ground band acquires greater curvature and the effective mass  $m^*$  decreases. The energy spacing between the  $k = 0$  state and nearby quasi momentum states increases proportionally to  $|k|$  in the extended zone scheme, which stabilizes the lowest state against small  $k$  excitations. Figure 6 illustrates the contrast between  $q = 2$  and  $q = 1$ . The reduction of  $m^*$  is strongest at smaller  $q$ , as summarized in Figure 7.

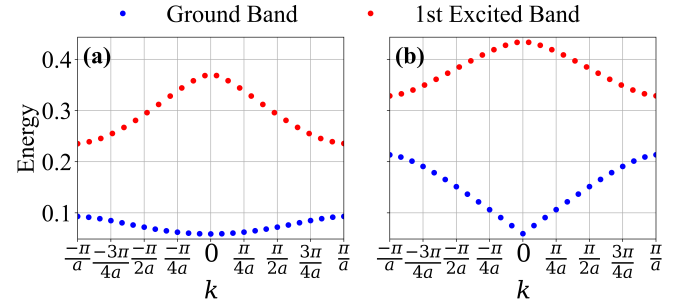


FIG. 6. (a)  $q = 2$ . (b)  $q = 1$ . Parameters:  $V_0 = 0.5$ ,  $L = 1.5$ ,  $W = 6.0$ . As  $q$  decreases, the spectrum shifts upward, the  $k = 0$  state rises more slowly than nearby quasi momentum states, and the ground-band curvature increases, yielding a monotonic decrease of  $m^*$  around  $k = 0$  for  $q < 2$ .

Figure 7 summarizes the effective mass  $m^*$  at the band minimum as  $q$  varies. The dispersion near  $k = 0$  dominates the response to  $q$ , so  $m^*$  decreases rapidly for  $q < 2$ , with the steepest drop as  $q \rightarrow 1$ . The logarithmic vertical axis highlights this rate of decrease.

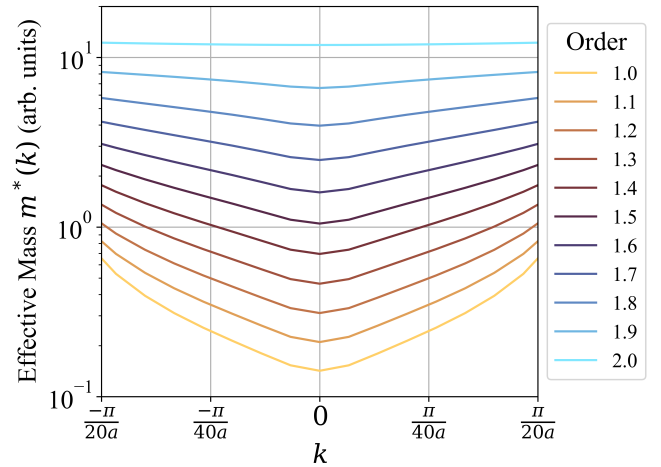


FIG. 7. Parameters:  $V_0 = 0.5$ ,  $L = 1.5$ , and  $W = 7.0$ .  $m^*$  is extracted from the curvature of the ground band around  $k = 0$ ,  $m^{*-1} = \partial_k^2 E|_{k=0}$ . As  $q$  decreases,  $m^*$  drops rapidly, appearing near-exponential in  $q$  on the log scale.

For  $q < 2$ , the effective mass at  $k = 0$  decreases nearly exponentially as  $q$  departs from 2. The rate of decrease

depends on geometry through  $V_0$ ,  $L$ , and  $W$ , with this dependence strongest near  $q \approx 2$  and weak as  $q \rightarrow 1$ . Across all tested potentials, the trend saturates at  $q = 1$  with  $m^* \approx 0.15 \pm 0.01$  and a maximum variance  $\leq 0.06$ . The lighter mass increases group velocity and mobility at fixed scattering time, enlarges coherent transport windows and tunneling rates in 1D superlattices, and therefore gives  $q$  a direct lever on low-field conductivity without changing the lattice geometry.

## V. CONCLUSION

Fractional order  $q$  provides a compact control axis for one-dimensional periodic quantum media, reshaping both band curvature and topology. Two regimes emerge, separated at  $q = 2$ . In the  $q > 2$  region, the band topology is changed via a symmetry-breaking inversion, creating a Bloch momentum qubit with logical states at symmetric valleys  $\pm k_{\min}$ . Valley position is tunable by  $q$  and potential geometry, and the inversion-completion point follows  $q \propto V_0^{-0.28 \pm 0.05} L^{-0.35 \pm 0.08} W^{-0.49 \pm 0.06}$ . When the first excited band does not invert concurrently, the gap develops a kink and the directness changes, which modifies optical coupling and relaxation pathways

[22, 23]. In contrast, for  $q < 2$ , the ground band sharpens around  $k = 0$ , causing a monotonic decrease in effective mass with  $q$ . The rate of this depends on the well geometry, where the dependence is strongest when  $q \approx 2$  and weakest as  $q \rightarrow 1$ . Across all tested potentials, the trend saturates at  $q = 1$  with  $m^* \approx 0.15 \pm 0.01$  and a maximum variance  $\leq 0.06$ .

Beyond the present one-dimensional stationary setting, higher-dimensional periodic systems may host richer  $q$ -driven dispersions, including Mexican-hat profiles [24]. Platforms that realize Lévy-flight transport offer experimental routes to probe the predicted band transformations, while time-domain studies of the Bloch momentum qubit can assess coherence, control, and device relevance.

These results establish fractional order  $q$  as a practical design lever that couples cleanly to geometry, yields falsifiable signatures in dispersion and gap directness, and interfaces with standard transport and optical readouts. The framework is applicable across one-dimensional periodic quantum media, providing immediate paths from theory to measurement and a new route to device-level control.

*Acknowledgments.*—This work was performed in part with support by the U.S. National Science Foundation under grants DMR-2002980, DGE-2125899, PHY-2210566, and PHY- 2515059.

---

[1] N. Laskin, Fractional quantum mechanics and lévy path integrals, *Physics Letters A* **268**, 298 (2000).

[2] N. Laskin, Fractional quantum mechanics (World Scientific Publishing Co. Pte. Ltd., 2018) pp. 23–65.

[3] B. Berkowitz, A. Cortis, M. Dentz, and H. Scher, Modeling non-fickian transport in geological formations as a continuous time random walk, *Reviews of Geophysics* **44**, 10.1029/2005RG000178 (2006).

[4] S. Longhi, Fractional schrödinger equation in optics, *Opt. Lett.* **40**, 1117 (2015).

[5] Y. Zhang, H. Zhong, M. R. Belić, and et al., Propagation dynamics of a light beam in a fractional schrödinger equation, *Physical Review Letters* **115**, 180403 (2015).

[6] G. M. Viswanathan, S. V. Buldyrev, S. Havlin, M. G. E. da Luz, E. P. Raposo, and H. E. Stanley, Optimizing the success of random searches, *Nature* **401**, 911 (1999).

[7] D. Brockmann, L. Hufnagel, and T. Geisel, The scaling laws of human travel, *Nature* **439**, 462 (2006).

[8] J. M. Lewis and L. D. Carr, Exploring multiscale quantum media: High-precision efficient numerical solution of the fractional schrödigner equation, eigenfunctions with physical potentials, and fractionally-enhanced quantum tunneling (2024).

[9] C. E. Rasmussen and C. K. I. Williams, *Gaussian Processes for Machine Learning* (MIT Press, 2006).

[10] S. A. Vitale, Valleytronic information processing and applications (2019), 2019 NSF/DOE/AFOSR Quantum Science Summer School.

[11] R. P. Feynman and A. R. Hibbs, *Quantum Mechanics and Path Integrals* (McGraw-Hill, 1965).

[12] D. J. Griffiths, *Introduction to Quantum Mechanics*, 2nd ed. (Pearson Prentice Hall, 2005).

[13] A. Caldeira and A. Leggett, Path integral approach to quantum brownian motion, *Physica A: Statistical Mechanics and its Applications* **121**, 587 (1983).

[14] V. Zaburdaev, S. Denisov, and J. Klafter, Lévy walks, *Reviews of Modern Physics* **87**, 483 (2015).

[15] R. Metzler and J. Klafter, The random walk’s guide to anomalous diffusion: a fractional dynamics approach, *Physics Reports* **339**, 1 (2000).

[16] C. Kittel, *Introduction to Solid State Physics*, 8th ed. (Wiley, 2004).

[17] M. Ameri, D. Rached, M. Rabah, R. Khenata, N. Benkhetou, B. Bouhafs, and M. Maachou, Structural and electronic properties calculations of bexzn1 xse alloy, *Materials Science in Semiconductor Processing* **10**, 6 (2007).

[18] P. R. Stinga, Fractional derivatives: Fourier, elephants, memory effects, viscoelastic materials and anomalous diffusions (2022).

[19] D. H. McIntyre, Quantum mechanics a paradigms approach (Pearson Addison-Wesley, 2012) Chap. 15 Periodic Systems, pp. 469–498.

[20] T. Robens, Models with (broken) z2 symmetries (2021).

[21] C. Hughes, J. Isaacson, A. Perry, R. F. Sun, and J. Turner, What is a qubit?, in *Quantum Computing for the Quantum Curious* (Springer International Publishing, Cham, 2021) pp. 7–16.

[22] S. Sze and K. K. Ng, Physics and properties of semiconductors—a review, in *Physics of Semiconductor Devices* (John Wiley & Sons, Ltd, 2006) Chap. 1, pp. 5–75.

[23] M. C. Peter Y. Yu, Vibrational properties of semiconduc-

tors, and electron-phonon interactions, in *Fundamentals of Semiconductors* (Springer Berlin, Heidelberg, 2010) pp. 107–158.

[24] V. Damjanović, Existence of mexican-hat dispersion and symmetry group of a layer, *Physica E: Low-dimensional Systems and Nanostructures* **170**, 116224 (2025).